Experimental investigation on load bearing and failure behavior of geosynthetic reinforced base courses of working platforms for mobile construction machines

Rainer Worbes & Christian Moormann
Institute for Geotechnical Engineering, University of Stuttgart, Germany

ABSTRACT: In a variety of construction projects, e.g. the construction of wind power plants and deep foundations, heavy working machines must be used on soft and low-bearing ground. In context of the research project "Bearing Layers for mobile Construction Machines and Cranes" the failure mechanism of geosynthetic reinforced multi-layered systems and the complex interaction between construction machines and supporting layers have been clarified by coupling model tests, field tests and numerical simulations. The performed 1g-model tests simulate the loading of construction machines on reinforced support layers underlain by a soft layer under static and cyclic loading conditions in the scale 1:3. This paper presents the results of model tests comparing the bearing and deformation behavior of reinforced and an unreinforced supporting layers for working platforms.

Keywords: Working platform, machine stability, reinforced bearing layer, load-bearing capacity, physical modeling, cyclic loading

1 INTRODUCTION

For the use of heavy mobile construction machines, e.g. drilling and trench wall units, rams, vehicle and crawler cranes, temporary working platforms are often created in the form of poured and compacted earth building materials, which are partially reinforced with geosynthetics. Particularly in the case of heavy working machines, the bearing capacity of the underlying subgrade is often insufficient to ensure a safe and usable installation considering all relevant operating and loading conditions. In a variety of construction projects, e.g. construction of wind power plants and deep foundations, heavy working machines are to be used on soft and low bearing ground. The use of working platforms and their correct dimensioning are therefore of fundamental importance for the durability of the construction machines and thus for work safety. In this context, there is a need for optimization, since the requirements of the construction machines are often not in line with the working platform design, and there are no commonly accepted technical regulations available for designing temporary working platforms made of unreinforced and reinforced supporting layers. Aim of the research project, initiated by the Institute for Geotechnical Engineering at the University of Stuttgart, is the development of a design approach able to guarantee a safe and usable installation of mobile machinery under construction site conditions. Based on the acquired knowledge, a recommendation for the dimensioning, construction, testing and maintenance of temporary working platforms shall be derived, that should be able to optimize working platform design both from technical and economical point of view. The research strategy is based on experimental and numerical investigations. The numerical simulation models are validated by measured data obtained from large-scaled model tests and real scale field tests. Based on a numerical parameter study, the influence of geometric and geotechnical parameters is investigated to gain an improved understanding of the bearing and deformation behavior of reinforced two-layer systems.

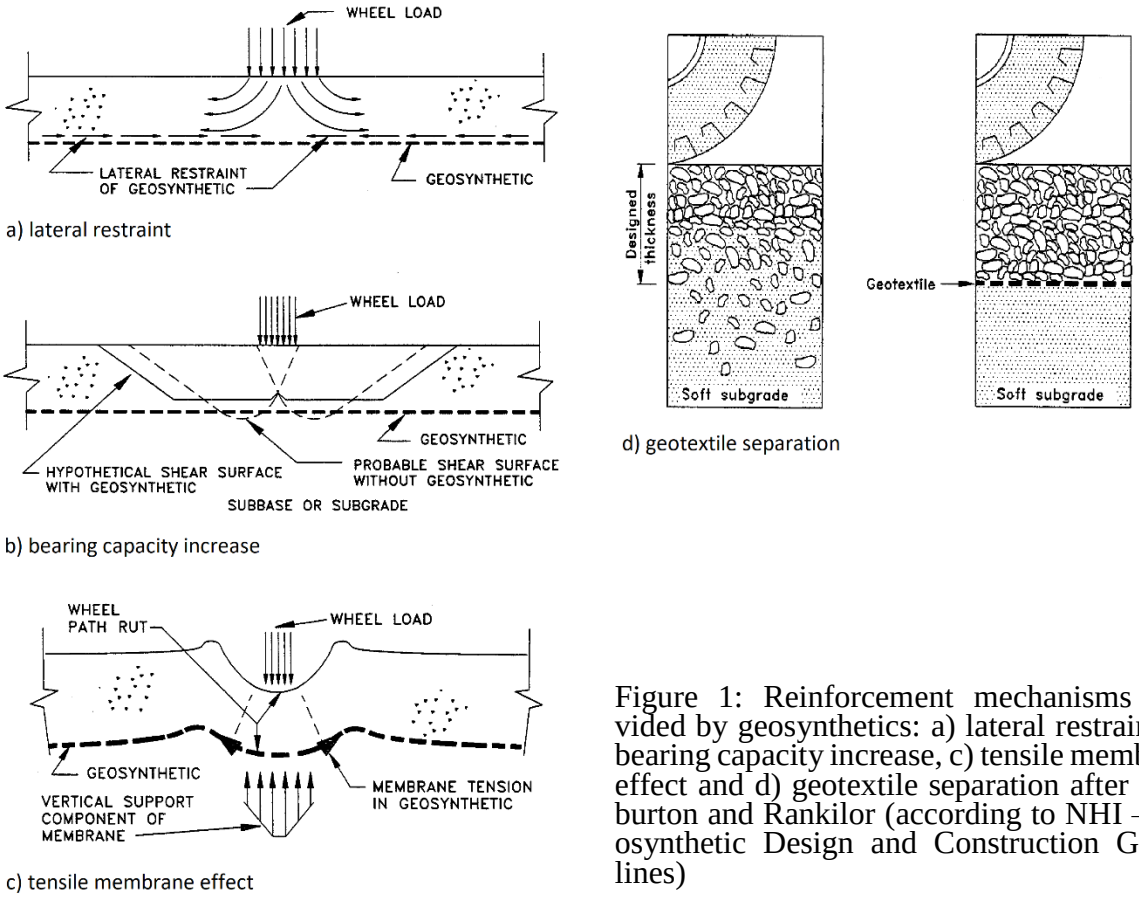

Figure 1: Reinforcement mechanisms provided by geosynthetics: a) lateral restraint, b) bearing capacity increase, c) tensile membrane effect and d) geotextile separation after Haliburton and Rankilor (according to NHI – Geosynthetic Design and Construction Guidelines)

2 LOAD-BEARING MECHANISMS OF GEOSYNTHETIC REINFORCED BASE COURSES

The load-bearing behavior of geosynthetic reinforced base courses under static and non-monotonous loading conditions is defined by several interaction mechanisms between the geosynthetic, the aggregate layer and the subgrade. There are four different load-bearing mechanisms discussed in literature, which can be identified for increasing the overall bearing capacity and durability of base course systems [Bender & Barnberg (1978), Giroud & Bonaparte (1984), Perkins & Ismeik (1997), Koerner (2012)].

2.1 *Lateral restraint*

Load spreading as a result from vertical loading induces additional lateral tension in the aggregate layer directly under the load plate. An unreinforced aggregate layer has practically no tensile strength, so that the aggregate layer tends to deform laterally, unless it is restrained by the subgrade. In unreinforced systems these horizontal displacements deteriorate the base course by increasing the void ratio and the thickness of the aggregate. Using geosynthetic reinforcements made from nonwovens or geogrids placed inside the aggregate layer or at the interface between both layers is able to transfer the lateral stress by frictional interaction and interlocking of the gravel inside the geogrid apertures. This additional lateral restraint increases the mean stress and acts like a confinement of the aggregates under the load plate, what reduces horizontal displacements and the associated reduction thickness and stiffness in the base course.

2.2 *Increasing bearing capacity*

Another effect is the influence of geosynthetic reinforcements on the shape of the shear surface in the soil body. Without geosynthetic reinforcement the potential failure surface, which consist of punching shear and local shear failure, will be partially developed in the subsoil, what leads to low bearing capacities. The potential bearing capacity failure surface of the reinforced system will be forced to develop only in the base course which consists of aggregates with a significantly higher friction angle and shear strength. This changes the failure mechanism from general and local shear failure to a punching shear failure, what increases the bearing capacity of the base course system.

2.3 *Tensile membrane effect*

The third load-bearing mechanism assumes the geosynthetic acting as a tensile membrane. The so called tensile membrane effect results from vertical displacements of the geosynthetic under the load plate, what leads to an additional vertical component of the tensile fore in the reinforcement and thus to an increase of the bearing capacity of the whole system. This effect requires a minimum of plastic deformation to take place and increases with additional settlements until the ultimate tensile force in the geosnythetic is reached and it rips. The tensile membrane effect transfers the vertical stress to areas outside the assumed load spread angle, which is marked by the punching shear failure surfaces in the base course. Additional vertical stress on the subsoil in the side areas additionally increases the bearing capacity of the subsoil itself, due to higher theoretical overloading.

2.4 *Separation effect*

Another effect is the geotextile separation in the interface between base course and subsoil. This effect is only reached by using nonwoven geosynthetics and woven geotextiles with small apperture size. The geosynthetic prevents the mixing between both materials. Fines from the subsoil can migrate into the aggregate layer by the pumping effect, what leads to reduced shear parameters. In addition, non-monotonous (cyclic, dynamic) loading conditions cause aggregates to be pushed into the fine grained soft soil of the subgrade, what results in lowering the thickness and stiffness of the base course.

3 ANALYTICAL DESIGN APPROACHES FOR REINFORCED BEARING LAYERS

For the dimensioning of unreinforced and reinforced working platforms, various approaches according to EBGEO, Giroud & Nioray, Meyerhof, Okamura and BR BRE 470 for determining the bearing capacity of two-layer systems made of aggregate layer and soft subsoil are available in literature. These are mainly based on the principle of load distribution or reduction on the underlying subgrade. In this case, the assumption is usually that the height of the supporting layer and the shear strength are chosen in such way, that a basic fracture failure occurs exclusively in the soft layer. The design approaches are based on the verification of the general bearing-capacity of single layered systems, by considering the load distribution and load reduction resulting from the aggregate layer. Only a few methods take into account the contribution of geosynthetics, and even then only in a very simplified manner respectively for some idealized conditions (single layer, constant spacing between layers, etc.). In some design methods, the required thickness of the supporting layer can be calculated directly.

4 EXPERIMENTAL CONCEPT

Using geotechnical model tests, allows to obtain deepened soil mechanic findings of the load-bearing and deformation behavior of unreinforced and reinforced supporting layers over subsoils with low stiffness, under static and cyclic loading conditions. Aim of the experimental test concept hereby is to investigate the

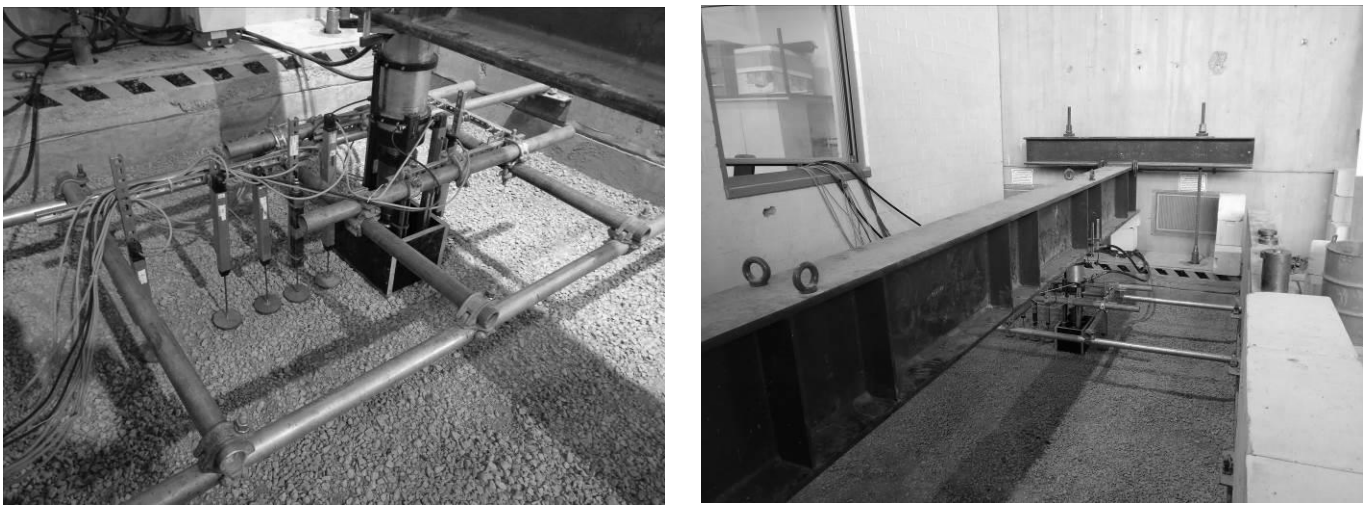

Figure 2: Setup of the model tests with actuator and potentiometric transducers (left) and testing field with reaction frame.

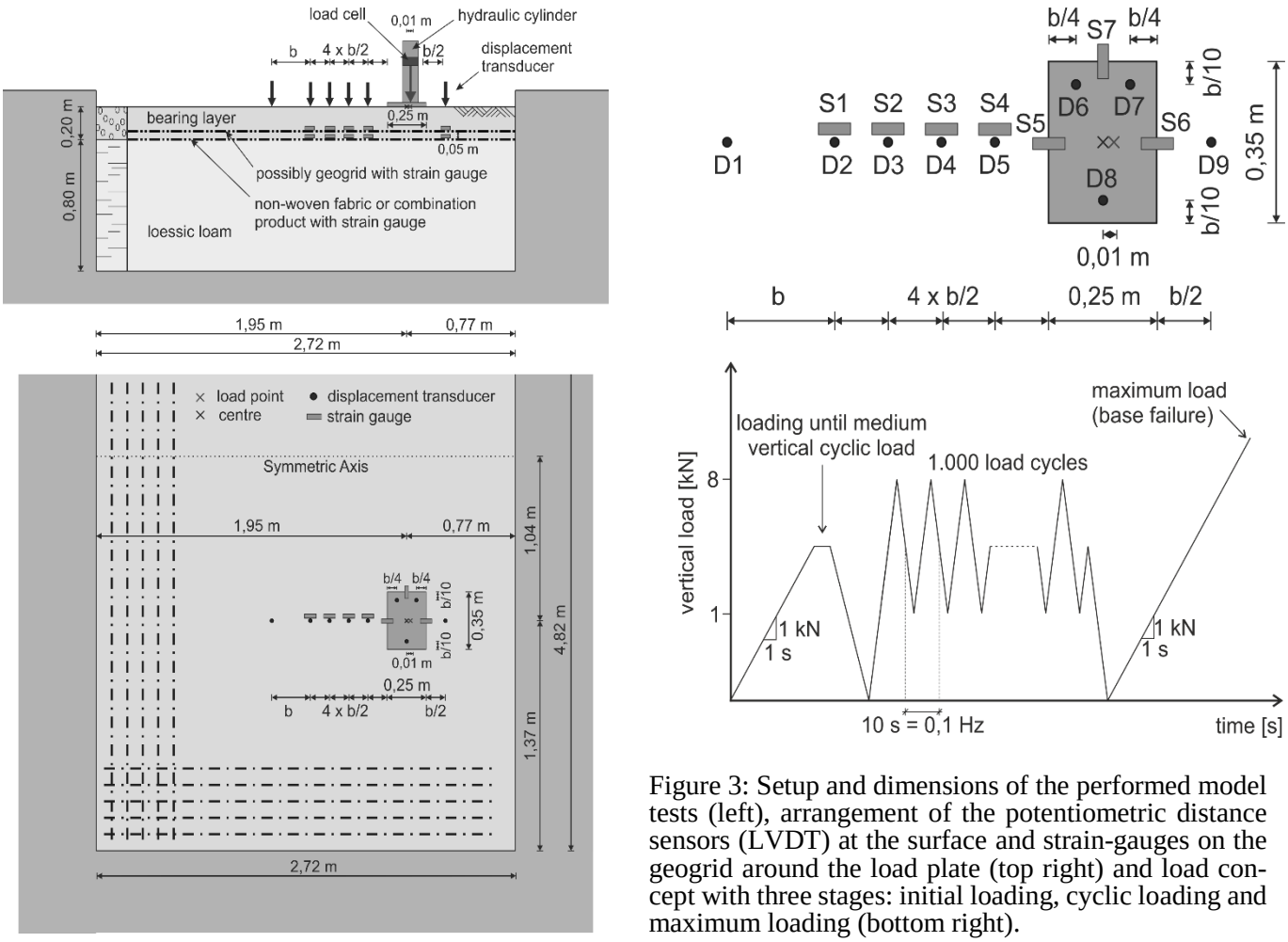

Figure 3: Setup and dimensions of the performed model tests (left), arrangement of the potentiometric distance sensors (LVDT) at the surface and strain-gauges on the geogrid around the load plate (top right) and load concept with three stages: initial loading, cyclic loading and maximum loading (bottom right).

failure mechanism (fracture and punching figure and mobilized shear planes) of unreinforced and reinforced two-layer systems. The serviceability states are represented by realistic load assumptions, frequencies and load cycle numbers of typical construction machines. Furthermore, the influence of geogrid reinforcement and the geogrid-behavior is investigated during load transfer, by measuring the strain development in the reinforcement. The findings to be gained on this basis are fundamentals for technically and economically optimized design approaches.

4.1 *General testing setup*

The geotechnical model tests are conducted as 1-g tests on 1:3 scale. Figures 2 and 3 illustrate the geometry and the arrangement of the measuring sensors of the experiment. The basal area of the test field is 4.82 m x 2.72 m, in which two model tests can be conducted separately from each other. Each test field has the dimensions 2.41 m x 2.72 m. The subgrade, represented by a layer of loess loam (SC/CL classification according to USCS) with an undrained shear strength c_u of 20 kN/m², has a thickness of 0.80 m. The soil parameters of the densified loess loam are controlled by the moisture content and the undrained shear strength is measured by in-situ vane shear tests. Above the soft layer, the aggregate layer is installed with a thickness of 0.20 m. For the installation of the bearing layer a well-graded sand-grit mixture with a grain size varying between 0 mm and 16 mm is used. The gravel mixture is incorporated with the proctor density of D_{Pr} = 100%. The size of the load plate is 35 cm x 25 cm (l x b), and the vertical test load is applied with an eccentricity e = 0.04 x b = 1 cm relative to the shorter foundation side to provide the direction of the basic fracture. Deformations on the surface are measured by linear variable differential transformers (LVDT) at nine points. In the reinforcement test, the strains in the geogrid are additionally measured at seven points by strain gauges. In the unreinforced test, a nonwoven is used as a separating element between the soft layer and the aggregate layer . It can be assumed that the nonwoven geosynthetic membrane, has only a minor reinforcement function, which can be neglected. For the reinforcement of the second test a composite product made of a biaxial geogrid (laid, welded knots) with a maximum tensile strength of 30 kN/m and a nonwoven, which is also used in the unreinforced experiment, was used. The combination product has also been placed between the soft layer and the bearing layer fulfilling both the functions of reinforcing and separating.

4.2 *Loading scheme*

The loading scheme, shown in Figure 3 can be divided into three different stages. The first stage is the monotonous loading phase, in which load is initially increased to the average cyclic load with a velocity of 0.1 kN/s. This causes plastic deformations prior to the cyclic loading stage and gives information about the initial stiffness. After that, the relief starts and the second stage, the cyclic loading, which simulates load effects under operating conditions, begins. In the second stage 1000 load cycles with a frequency of 0.1 Hz and an amplitude of 3.5 kN between 1 kN and 8 kN were applied. During the final stage, the load is increased up to a defined failure state, in order to obtain the ultimate bearing capacity.

5 TESTING RESULTS

In the following, the results of an unreinforced and a reinforced test are presented and compared to analyze the influence of the geogrid reinforcement in terms of stiffness and load-bearing capacity.

5.1 *Cyclic loading*

Figure 4 shows the vertical settlement of the load plate during cyclic loading on the unreinforced and on the reinforced supporting layer. Obviously, the unreinforced bearing layer initially deforms more strongly, but for the cyclic load there is only a small difference in the accumulation of permanent deformations recognizable. A reason therefore is the influence of the separation effect of the nonwoven in both systems. The settlement of the load plate has almost doubled in both systems, compared to the initial load, after about 1000 load changes. The reinforced system shows greater deformations intervals for each load cycle, and therefore a larger elastic deformation region.

5.2 *Settlement and bearing capacity*

Figure 4-b shows the comparison of the load-settlement curves of the load plate for the unreinforced and the reinforced system in case of static load applied after the cyclic load. The stiffness of both two-layer systems is comparatively high up to almost 16 kN and there is almost no significant increase of the deformation. The main reason for this is the compression by the cyclic preload with a maximum load of 8 kN during stage two. At approximately 56 kN, the load plate is relieved due to the maximum press stroke in the unreinforced system. The relief shows high plastic deformations of 15 cm. The plate is then reloaded again and the maximum bearing capacity is reached at 67.6 kN. The settlement of the load plate increases from 24 cm to almost 30 cm, although the load decreases and the system fails. The reinforced system initially has the same stiffness. The geogrid reinforcement requires sufficient deformation and settling to activate tensile forces. From about 30 kN the stiffness is significantly higher compared to the unreinforced system. The relief due to the maximum press stroke is at a load of approximately 80 kN. The plastic deformation of the bearing layer under the load plate is about 15 cm, which corresponds to the unreinforced system, although the load was about 45% higher. The maximum load is reached at 82.5 kN. The settlement of the load plate increases from 27 cm to 30 cm, although the load decreases. The maximum settlement of

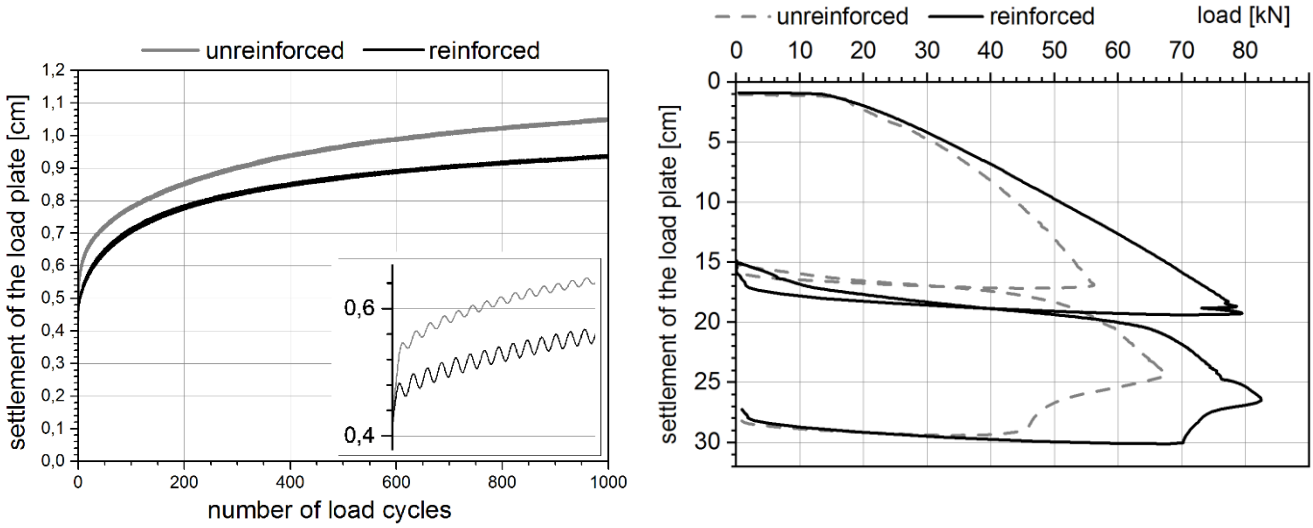

Figure 4: Comparison of the settlement of the load plate on the reinforced and unreinforced support layer for cyclic loading (left) and for maximum loading (right).

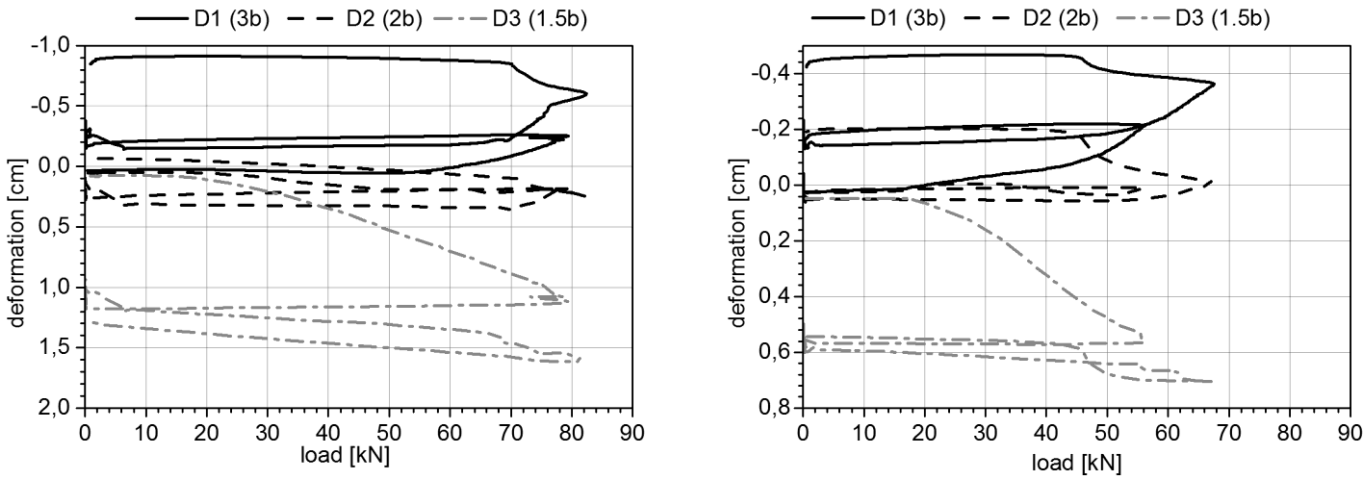

Figure 5: Comparison of the settlement of the load plate for the measuring points D1 to D3 for the unreinforced (left) and the reinforced test (right).

both systems is almost identical, while the bearing capacity of the reinforced system is 22% higher than the system with an unreinforced base layer. Figure 5 shows the vertical displacement on the surface of the bearing layer at the measuring points D1 (3b), D2 (2b) and D3 (1.5b) for the unreinforced supporting layer (location of the points according to Figure 3. Positive deformations mean lowering and negative deformations mean lifting. The measuring points D1 to D3 are located farthest from the load plate and thus less influenced by the subsidence cavity. At the beginning of the static loading phase, settlements are already present at the point D1 because of the first static and the cyclic preload. After a small increase of the load, the supporting layer begins to heave. After reaching the ultimate failure load, further lifting occurs, although the load decreases. Point D2 shows almost neglectible deformation up to the maximum load. Once the maximum load-bearing capacity is reached, the ground heaves by 0.2 cm. Point D3 shows increasing settlements from the beginning for both tests. The load-deformation envelopes at the measurement points D1 (3b), D2 (2b) and D3 (1.5b) for the reinforced system are shown in Figure 5. The displacements of the point D1 are affine to the unreinforced system, but the elevations are significantly higher. At the application of the vertical load, the ground settles at point D2. When reaching the ultimate capacity, the aggregate layer starts lifting slightly, due to the volume constant displacements. At the distance of 1.5b at point D3, the settlements are significantly greater than in the unreinforced system. The larger deformations for the reinforced system for this area can be explained by increasing the range of the subsidence cavity, due to the load spreading and the tensile membrane effect of the geogrid reinforcement. Figure 6 illustrates the vertical deformation along the measurement axis for the points D1 to D9 for the unreinforced and reinforced bearing layer. The settlement of the load plate is calculated from the results of the transducers D6 and D7. The

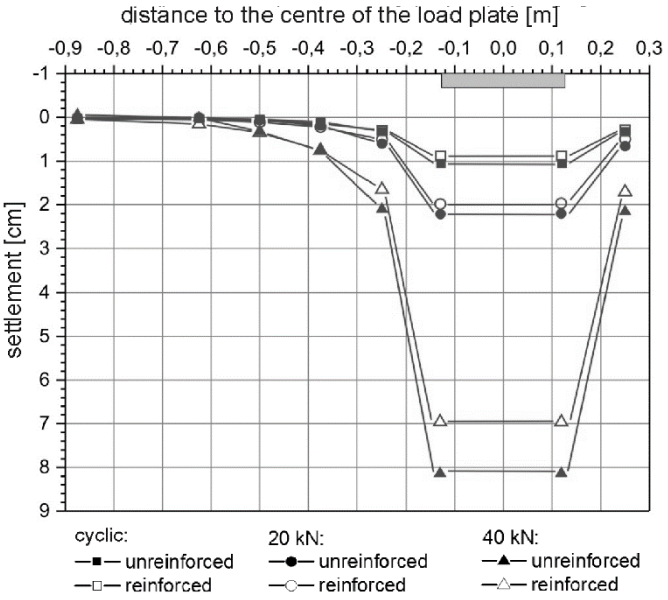

Figure 6: Comparison of the settlement of the load plate and on the surface on the reinforced and unreinforced support layer along the measuring cross section for unreinforced and reinforced supporting layers (left), arrangement of the potentiometric transducers (right).

deformation after the cyclic loading is approximately the same for loading until 20 kN, although the deformation for the reinforced system is slightly lower. As the load is increased, the difference between both systems becomes more significant, due to the progressing activation of the Geogrid reinforcement and the tensile membrane effect. The influence of this effect is locally limited to a range of about 1.5b around to the load plate, due to the punching of the load plate into the sub layer.

5.3 *Strain development*

The measured strains in the geogrid reinforcement along the measuring axis of the second test are shown in Figure 7-a. It can be noticed that the strain in the geogrid are very small for lower loading conditions up to 20 kN (25% of the bearing capacity) and remain limited to a range of 1.5b distance around the center of the load plate. At approximately 30 kN, a significant increase in strain is achieved at all measuring points. With an increase in load to 40 kN, strain on all measuring points increases disproportionately. The geogrid reinforcement at the peripheral strain-gauges S1 to S3 is activated much later, so that in contribution of these areas in transferring the load larger vertical deformations of the reinforcement are required. The strains up to the load of 20 kN largely correspond to the lateral restraint forces due to horizontal load distribution, whereas the strain is additionally superimposed by the increasing tensile membrane effect. Figure 7 shows the development of tensile strain in the geogrid reinforcement over the plate load and for the strain-gauges S1 to S7. At the beginning of loading phase three, the strain-gauges S5, S6 and S7, located the edge under the load plate receive the highest strain ratio. The strain-gauge S7 is located perpendicular to the measuring axis at the load plate, what results in lower strain ratio increasing until about 25 kN. Then the punching shear failure of the subsoil begins and the geosynthetic receives additional strain close to the load plate. The eccentricity of the load plate in the direction of S6, leads to a minimum higher strain ratio than at S5. Strain-gauge S4, which is located at the distance of 12.5 cm from the edge of the load plate, receives to almost 1% elongation only 60 % of the strain from S5 and S6. This is an indicator for the dominance of the lateral restraint effect, with increasing strain towards the center of the load plate. Until reaching about 15 kN, the strains in the geogrid reinforcement at the strain-gauges S1 to S3 decrease resulting from axial compression, due to lateral displacements of the soft soil in this area. The displacements result from lateral horizontal stress under the load plate and the partially undrained deformation behavior of the soft soil. Undrained behavior is manifested by volume-constant changes in shape. Activation of the tensile force in the geogrid increases step by step from S1 to S6, due to higher influence of the tensile membrane effect, which affords an increased anchored length of the geosynthetic. The tensile membrane effect additionally superimposes the lateral restraint effect at about 15 kN until reaching the maximum bearing capacity.

6 FAILURE MECHANISM

The failure mechanism consists of a combination of punching shear failure of the aggregate layer and the base failure of the subgrade. In the case of unreinforced system, the base failure takes place after perforation of the supporting layer. Due to the low shear strength of the soft layer, there occurs no general shear failure,

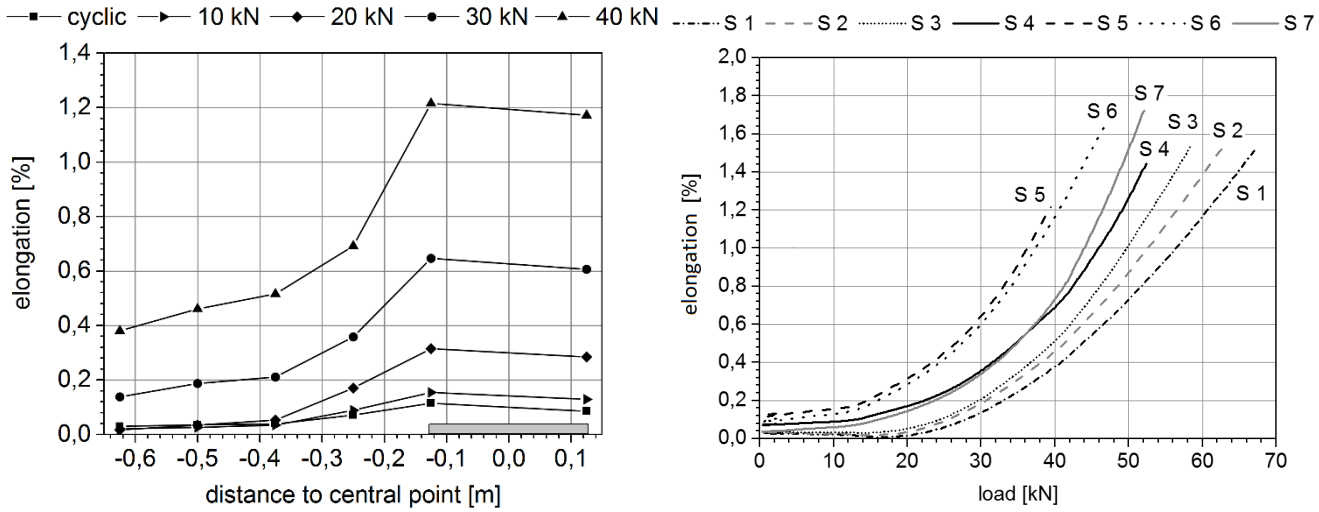

Figure 7. Measured strains on the geogrid reinforcement between the supporting layer and the subgrade: development along the measured cross section (left), elongation over load (right).

so that the failure mechanism changes to a punching shear failure with increasing deformations. For the reinforced system both mechanisms, the perforation of the support layer and the punching shear failure take place long before the reinforcement fails. The final failure state, from which no further increase of the vertical load is possible, is marked by the rupture of the geogrid. The geogrid used in the test rips under the edge of the load plate, due to the increasing tensile forces in this area. The range of the subsidence cavity of the unreinforced system is limited to the range of about 1b, while the sides are much steeper than in the reinforced system. In the reinforced systems the flanks of the subsidence cavity are less steep, but the range is much wider (2b). The tensile membrane effect begins to superimpose the lateral restraint effect at about 0.5 to 1.5 % elongation, due to higher strain rations from the increase of the vertical force component resulting from additional loading.

7 CONCLUSION

The comparison between a non-reinforced and a reinforced support system in the small-scale model tests shows that the maximum bearing capacity can be significantly increased with a geogrid reinforcement. The reinforcement improves the deformation behavior, especially at higher loads due to the load spreading of the tensile membrane effect. The strain measurements show that geogrid-reinforcements clearly optimize the load and deformation behavior. Bearing capacity in this case is increased about 22% and the settlements at the load plate are reduced from 10% to 15%. For low stress conditions, both the unreinforced and reinforced system show similar deformation behavior. This depends on the minimum of deformation that is necessary for activating the geogrid reinforcement. The geogrid reinforcement also increases the elastic deformation region for unloading and reloading cases for e.g. in cyclic loading conditions. In context of the research project further model scale tests with various parameter setups are conducted. Parameters to be examined are: the influence of the height of the support layer, the shear strength of the soft layer and other influencing factors of the reinforcement like tensile stiffness, arrangement and type of the geosynthetics.

REFERENCES

Bender, D.A. & Barnberg, E.J. 1978. Design of soil-fabric-aggregate system. Transportation Research Record 671, pp. 64-75.

BRE - Building Research Establishment 2004/2007. Working platforms for tracked plant: good practice guide to the design, installation, maintenance and repair of ground-supported working platforms (BR 470). IHS BRE Press, Bracknell, Berkshire, ISBN 186081 7009.

Deutsche Gesellschaft für Geotechnik / German Geotechnical Society 2010. Empfehlungen für den Entwurf und die Berechnung von Erdkörpern mit Bewehrungen aus Geokunststoffen – EBGEO, 2nd Edition, Berlin: Ernst & Sohn.

Deutsches Institut für Normung / German Institute for Standardization 2006. DIN 4017:2006-03 "Baugrund - Berechnung des Grundbruchwiderstands von Flachgründungen".

Giroud, J.-P., Ah-Line, C., and Bonaparte, R. 1984. Design of unpaved roads and trafficked areas with geogrids. Polymer Grid Reinfocement, A conference sponsored by SERC and Netlon, Ltd., Thomas Telford, London, England, pp. 116-127.

Giroud, J.-P. & Noiray, L. 1981. Geotextile-Reinforced unpaved road design. Journal of the Geotechnical Engineering Division Vol. 107 (No. GT9), pp. 1233–1254.

Haliburton, T.A., Lawmaster, J.D., McGuffey, V.C. 1981, Use of Engineering Fabrics in Transportation Related Application, FHWA DFH61-80-C-00094.

Koerner, R.M. 2012. Designing with Geosynthetics, 6th Edition, New Jersey, Pearson Prentice Hall, Upper Sadle River.

Lehn, J., Moormann, C. 2016. Invesigations on a geosynthetic reinforced bearing layer under static and cyclic loading. 19th International Conference on Soil Mechanics and Geotechnical Engineering, Seoul, South Korea.

Meyerhof, G. G. 1974: Ultimate bearing capacity of footings on sand layer overlying clay. Canadian Geotechnical Journal Vol. 11 (No. 2.): pp. 223–229.

National Highway Institute: Geosynthetic Design and Construction Guidelines 1998, DTFH61-93-C.00120, Washington, D.C., United States of America.

Okamura, M., Takemura, J., and Kimura, T. 1997. Centrifuge Model Tests on Bearing Capacity and Defomation of Sand Layer Overlying Clay, Soils and Foundations, Vol. 37(1), pp. 73-88.

Perkins, S.W. & Ismeik, M. 1997. A Synthesis and Evaluation of Geosynthetic-reinforced Base Course Layers in Flexible Pavements: Part I Experimental Work. Geosynthetics International, Vol. 4, No. 6, pp. 549-604.

Perkins, S.W. & Ismeik, M. 1997. A Synthesis and Evaluation of Geosynthetic-reinforced Base Course Layers in Flexible Pavements: Part II Analytical Work. Geosynthetics International, Vol. 4, No. 6, pp. 605-621.

Rankilor, P.R. 1981, Membranes in Ground Engineering, John Wile & Sons, Inc., Chichester, England, pp. 377.

Worbes, R., Moormann, C. 2018. Load-bearing and deformation behavior of unreinforced and reinforced model tests (German). 11th Colloquium – Construction in soil and rock, Technical Academy Esslingen, Germany.

Moormann, C., Lehn, J., Worbes, R. 2017. Reinforced bearing layers for working platforms of mobile construction machines and crane platforms - bearing behavior and optimization approaches (German). 10th Geosynthetic – Colloquium, Bad Gögging, Germany.